

MOL #111534

## Title Page

The temperature dependence of kinetics associated with drug block of hERG channels are compound specific and an important factor for proarrhythmic risk prediction.

Monique J. Windley, William Lee, Jamie I. Vandenberg, Adam P. Hill

Victor Chang Cardiac Research Institute, 405 Liverpool Street, Darlinghurst, NSW 2010,  
Australia (MW, WL, JV, AH)

St Vincent's Clinical School, University of NSW, Victoria Street, Darlinghurst, NSW 2010,  
Australia (MW, WL, JV, AH)

MOL #111534

## Running Title Page

**Running title:** Temperature dependence of hERG drug block kinetics

### Corresponding author:

Adam Hill

Molecular Cardiology and Biophysics Division

Victor Chang Cardiac Research Institute

405, Liverpool Street

Darlinghurst

NSW 2010

Australia

T: +61 2 9295 8686

F: +61 2 9295 8770

E: [a.hill@victorchang.edu.au](mailto:a.hill@victorchang.edu.au)

**Pages: 45**

**Tables: 3**

**Figures: 5**

**References: 24**

**Abstract words: 238**

**Introduction words: 657**

**Discussion words: 1570**

MOL #111534

**Abbreviations:** AP, action potential; APD, action potential duration; APD<sub>90</sub>, action potential duration at 90% repolarization;  $I_{Kv11.1}$ , Kv11.1 channel current;  $I_{Kr}$ , rapid component of delayed rectifier current; ECG, electrocardiogram; FDA, US Food and Drug Administration; CiPA, Comprehensive *In vitro* Proarrhythmic Assay, hERG, human Ether-à-go-go-related gene channel; RT, room temperature; CHO, Chinese hamster ovary; DMSO, dimethylsulfoxide; D + C, drug unbound channel; DC drug bound blocked channel; HT, high throughput, EAD, early after depolarization

MOL #111534

## Abstract

Current mandated preclinical tests for drug induced proarrhythmia are very sensitive, but not sufficiently specific. This has led to concern that there is a high attrition rate of potentially safe drugs that could have been beneficial to patients. The comprehensive *in vitro* proarrhythmia (CiPA) initiative has proposed new metrics based around *in silico* risk predictions, which are informed, amongst other things, by measures of hERG block kinetics. However, high throughput patch-clamp systems set to collect this data largely operate at ambient temperature, while the simulations for risk prediction are carried out at physiological temperature. The aims of this study were i) To determine to what degree kinetics of drug block of hERG are temperature dependent; ii) Assess the impact of any temperature dependence of drug binding kinetics on repolarization *in silico*; and iii) Identify whether a common set of  $Q_{10}$  scalars can be used to extrapolate kinetic data gathered at ambient to physiological temperatures for use in *in silico* proarrhythmic risk prediction. We show for a range of drugs that kinetics of block are temperature dependent and furthermore that the degree of temperature dependence is different for each drug. As a result, no common set of  $Q_{10}$  scalars could describe the observed range of temperature dependencies. These results suggest that if accurate physiological temperature models of the kinetics of drug binding are important for *in silico* risk prediction, the *in vitro* data should be acquired at physiological temperature.

MOL #111534

## Introduction

The human Ether-à-go-go-related gene (hERG) potassium channel carries the rapid delayed rectifier current ( $I_{Kr}$ ), one of the major repolarizing currents in the heart. Pharmacological block of hERG results in reduced repolarization, action potential (AP) prolongation, and an increased susceptibility to the fatal ventricular arrhythmia, *torsades de pointes*. It is estimated that ~70 % of all chemical compounds in preclinical drug development block hERG channels at some concentration (Shah, 2008). Consequently, regulatory guidelines mandate that all drugs must be tested for hERG potency and action potential (AP) prolongation (ICH S7B, Food and Drug Administration, 2005). These guidelines have been very successful in that no new proarrhythmic drugs have unknowingly been introduced to the market since their inception. However, it is now widely accepted that not all drugs that block hERG are dangerous (Aiba et al., 2005; Martin et al., 2004), meaning the current approach to screening potentially results in a high attrition rate of compounds that are in fact safe (Redfern et al., 2003; Sager et al., 2014; Yap and Camm, 2003). To address this concern, the US Food and Drug Administration (FDA) has proposed the Comprehensive in Vitro Proarrhythmic Assay (CiPA) (Sager et al., 2014). CiPA aims to develop a mechanism based risk score that is a more accurate predictor of proarrhythmia than the present metrics. CiPA will require assessing both the potency and kinetics of block of hERG (and other ion cardiac ion channels) in order to inform *in silico* models of the cardiac AP as tools to predict risk (Fermini et al., 2016; Sager et al., 2014).

In this regard, the kinetics of drug block have been shown to be an important contributor to the degree of prolongation observed in simulations of the effect of hERG blocking drugs on

MOL #111534

the cardiac action potential (Di Veroli et al., 2014; Lee et al., 2016). Furthermore, the kinetics of binding, as well as associated phenomena such as drug trapping are important measures required to inform *in silico* models of proarrhythmic risk (Li et al., 2017). Based on this requirement, a simple step based protocol was designed which balanced the ability to gather relevant kinetic information with the practical limitations of its application on high-throughput (HT) platforms (Windley et al., 2017). An important question that remains around the broad implementation of these protocols as part of a new preclinical screening approach is whether pharmacological data gathered using HT systems, which predominately operate at ambient temperature, can be usefully employed in developing *in silico* models of the effect of these drugs in physiological temperature action potential simulations. Specifically, there is a need to assess whether the kinetics of drug binding measured using the step depolarization protocol are temperature dependent, whether individual drugs have different temperature dependencies to their kinetics of binding, and whether a common scaling factor might be used to describe the effects of temperature on the kinetics of hERG block by different drugs.

The aims of this study were therefore to investigate whether the kinetics of drug block at ambient temperature was significantly different from that obtained at physiological temperature and/or whether there were consistent temperature dependent differences in kinetics for different drugs. To achieve this we used the Cytobatch automated patch-clamp system to collect kinetic and potency data, using the step depolarization protocol (Windley et al., 2016), for a number of drugs from the CiPA training panel. The kinetics of drug block were measured at both ambient (22 °C) and physiological (36°C) temperature and it was found that the kinetics of block for each of the drugs tested was significantly temperature

MOL #111534

dependent. By using a simple bi-molecular model of drug block the binding ( $k_{on}$ ) and unbinding ( $k_{off}$ ) rates were inferred and used to interrogate the impact of the temperature dependent kinetics on prolongation of the AP *in silico*. The results of this study suggest that the temperature at which drug block kinetics are recorded *in vitro* will have significant consequences for the accurate assessment of proarrhythmic risk.

MOL #111534

## Materials and Methods

### Cell culture

CHO cells stably expressing hERG/K<sub>v</sub>11.1 were purchased from the American Type Culture Collection (ATCC reference PTA-6812). Cells were cultured in Hams F12 nutrient mix (ThermoFisher Scientific, Waltham, USA) containing 5% fetal bovine serum (Sigma-Aldrich, Sydney, Australia) and maintained at 37 °C with 5% CO<sub>2</sub>.

### Patch clamp electrophysiology

#### Automated

Experiments were performed on the automated Cytopatch™ 2 system, unless stated otherwise (Cytobioscience, San Antonio, USA). Silicon dioxide microfluidic chips containing two embedded quartz pipette tips of 3-5 MΩ resistance were used to record two cells in parallel. The sequence of cell catching, sealing, whole-cell formation, capacitance correction and series resistance (~70%) compensation were all performed under automation using the Cytopatch. Whole cell patch clamp currents were evoked from CHO cells in the voltage clamp configuration at ambient temperature (22 °C) and physiological temperature (36°C). The current signal was amplified and filtered at 1 kHz and sampled at 10 kHz by the Cytopatch system (Cytobiosciences). Leak currents were subtracted manually offline. Data was acquired with the Cytopatch software (Cytobiosciences) and analysed using Clampfit (Molecular Devices) and Prism (v6, GraphPad, San Diego, USA).



MOL #111534

Pipettes were filled with internal solution containing (in mM): 100 potassium gluconate, 20 KCl, 2 Mg<sub>2</sub>ATP, 1 CaCl<sub>2</sub>, 1 MgCl<sub>2</sub>, 11 EGTA, 3 phosphocreatine, 9 sucrose and 10 HEPES, adjusted to pH 7.2 with KOH. The external bath solution contained (in mM); 140 NaCl, 5 KCl, 2 MgCl<sub>2</sub>, 2 CaCl<sub>2</sub>, 10 glucose and 10 HEPES, adjusted to pH 7.4 with NaOH. The calculated liquid junction potential of -15 mV (Barry, 1994) was corrected for by adjusting voltage pulse protocols prior to stimulation.

### **Manual**

For manual patch clamp experiments, whole cell patch clamp currents were evoked from CHO cells in the voltage clamp configuration at 22°C. The current signal was amplified and filtered at 1 kHz with an Axopatch 200B (Molecular Devices, Sunnyvale, USA) and sampled at 5 kHz with a PC interfaced with an analog to digital converter, Digidata1440A (Molecular Devices). Series resistance compensation was >80%. Leak currents were subtracted manually offline. Data was acquired with pCLAMP 10 (Molecular Devices) acquisition software and analysed using Clampfit (Molecular Devices) and Prism (v6, GraphPad, San Diego, USA).

Single use patch pipettes were pulled from borosilicate glass (Harvard Apparatus, Holliston, USA) with resistances of 2-5 MΩ. Pipettes were filled with internal solution containing (in mM): 120 potassium gluconate, 20 KCl, 1.5 Mg<sub>2</sub>ATP, 5 EGTA and 10 HEPES, adjusted to pH 7.2 with KOH. The external bath solution contained (in mM); 130 NaCl, 5 KCl, 1 MgCl<sub>2</sub>, 1 CaCl<sub>2</sub>, 12.5 glucose and 10 HEPES, adjusted to pH 7.4 with NaOH. The calculated liquid junction potential of -15 mV (Barry, 1994) was corrected for by adjusting voltage pulse protocols prior to stimulation.

MOL #111534

## **Drug application/Pharmacology**

The panel of drugs selected for this study were based on an original CiPA training panel of 12 drugs split equally between low, intermediate and high proarrhythmic risk, nominated by the CiPA Clinical Translation Working Group (CTWG) (Colatsky et al., 2016). From this panel, six drugs (verapamil, cisapride, bepridil, terfenadine, dofetilide and diltiazem) were chosen for this study. The first five of these was chosen since they were previously shown to have kinetics that could be accurately measured using the step depolarization protocol (Windley et al. 2017). Diltiazem was included as an example of a drug with kinetics too fast to measure at ambient temperature to assess whether the effect of temperature on gating kinetics relative to drug binding might actually improve our ability to measure binding kinetics for such drugs (Windley et al., 2017). Concentrations were selected from those previously examined (Windley et al., 2017). Only two concentrations were used for each drug due to the difficulties of measuring drug block kinetics at concentrations where block was minimal and/or too slow (data not shown). Where necessary for solubility, drugs were dissolved in DMSO. The maximum amount of DMSO never exceeded 0.1% (v/v), a concentration which has been shown to have no effect on hERG channel activity (Walker et al., 1999).

## **Data acquisition**

Data was acquired using the step depolarization protocol established by the CiPA Ion Channel Working group (ICWG) (Windley et al., 2017). Briefly, hERG channel currents were recorded using a step pulse starting from a holding potential of -80 mV followed by a step to the test potential of 0 mV for a period of 10 or 40 s based on the period required to reach

MOL #111534

drug block equilibrium (Supplementary Figure 1A(i)). The interpulse interval was 15 s, where cells were held at -80 mV. Five pulses were repeated in this manner in the absence of drug to assess current stability and to act as the control current. Following this the membrane was clamped at -80 mV where all channels exist predominantly in the closed state and subsequently the drug is unable to enter or block the channel, thus allowing drug equilibration to occur. This phase consisted of five 25 s or three 55 s -80mV pulses (dependent on whether the 10 s or 40 s 0 mV pulse protocol was in use, respectively) in the presence of drug perfusion (Supplementary Figure 1A(ii)). Finally, the 0 mV pulse was repeated to induce channel opening whereby the onset and potency of drug block was measured in the presence of drug perfusion (Supplementary Figure 1A(iii)).

### Data analysis

To measure the kinetics of drug block, the timecourse of the block onset was calculated through offline subtraction of data collected at 22 and 36°C:

$$\% \text{ block} = \left( \frac{i-ii}{i} \right) \times 100 \quad \text{Eqn 1}$$

Where  $i$  is the control current trace (no drug) and  $ii$  is the first trace in the presence of drug.

The percentage block data was fitted with a standard exponential function yielding a single time constant ( $\tau_{on}$ ):

$$f(t)_{on} = (I_m - I_d) \times (e^{-t/\tau_{on}}) + I_d \quad \text{Eqn 2}$$

Where  $I_m$  is the maximum percentage block at  $t = 0$ ,  $I_d$  is the percentage block plateau amplitude in the presence of drug,  $t$  is time,  $\tau_{on}$  is the time constant.

MOL #111534

## Modeling

Measured  $\tau_{on}$  values from hERG current responses were used to calculate the rate of drug association ( $k_{on}$ ) and rate of drug dissociation ( $k_{off}$ ). A simple bimolecular model of drug binding was used to describe the drug/hERG interaction:



Where D is drug, C is the channel in the open state and DC is the drug bound channel. Values for  $k_{on}$  and  $k_{off}$  were calculated for both 22 and 36°C using MATLAB 2016a software (Mathworks, Matlack, MA) to solve simultaneous equations of the form:

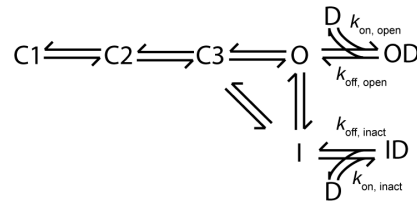
$$k_{on} \times [D_a] + k_{off} = 1/\tau_{on(a)} \quad \text{Eqn 3}$$

$$k_{on} \times [D_b] + k_{off} = 1/\tau_{on(b)} \quad \text{Eqn 4}$$

Where  $[D_a]$  and  $[D_b]$  are the two drug concentrations used, with  $\tau_{on(a)}$  and  $\tau_{on(b)}$  as their respective measured time constants. Calculated  $k_{on}$  and  $k_{off}$  values for 22 and 36°C were then used to simulate drug-induced prolongation of the cardiac AP.

Action potential simulations were performed using the O'Hara-Rudy 2011 model (ORD11) in its endocardial configuration (O'Hara et al., 2011). The description of  $I_{Kr}$  in ORD11 was replaced with the Markov state model shown in Scheme 2 (Lu et al., 2001) and this system was used to simulate the effects of drug binding to hERG on the cardiac AP.

MOL #111534



Scheme 2

Where D is drug, C1-3 are the closed channel states, O is the open state, I is the inactive state and OD and ID are the drug bound open and inactive channel states, respectively. For the sake of simplicity, drug binding ( $k_{on}$ ) and dissociation ( $k_{off}$ ) rates to the open and inactive state were considered to be equal.

For drugs that bind to multiple ion channels, dose-response curves of the form:

$$\frac{1}{1 + 10^{(\log[D] - \log(IC_{50})) * n}} \quad \text{Eqn 5}$$

were generated using published data from Crumb et al. (Crumb et al., 2016), where  $\log[D]$  is the logarithm of the drug concentration  $[D]$ ,  $IC_{50}$  is the 50% inhibitory concentration and  $n$  is the Hill coefficient for the drug in relation to a specific ionic channel. These concentration-response curves were then used to calculate the fraction of residual unblocked current for individual ionic channels and simulated as percentage of instantaneous block of that channel within the ORD11 model. Simulations were equilibrated for 300 beats with a cycle length of 1000 ms. The time to 90 percent repolarisation of the action potential duration ( $APD_{90}$ ) on the 300<sup>th</sup> beat of each simulation was calculated. All simulations and analysis were carried out using MATLAB software (Mathworks, Matick, MA).

For temperature dependent effects,  $Q_{10}$ , the factor by which the rate increases over a 10 °C temperature change was calculated according to the equation:

$$Q_{10} = \left(\frac{k_2}{k_1}\right)^{\left(\frac{10}{T_2 - T_1}\right)} \quad \text{Eqn 6}$$

MOL #111534

Where  $k_1$  and  $k_2$  are the reaction rates measured at temperatures  $T_1$  and  $T_2$  respectively.

### **Statistical Methods**

Statistical comparisons between groups were made using Mann-Whitney test. Since  $n$  numbers were insufficient to make assumptions about the distributions of variables, a non-parametric test was deemed appropriate. Measurement of kinetics and degree of block at ambient and physiological temperature were not carried out in the same cells, so an unpaired test was used. A  $p < 0.05$  was considered significant.

### **Chemical compounds**

All chemicals were supplied by Sigma-Aldrich (Sydney, Australia) unless otherwise stated.

MOL #111534

## Results

### Temperature dependence of drug block

The timecourse of the onset of drug block was initially measured for all drugs using the 10 s 0 mV step depolarization protocol on the automated Cytospatch platform at ambient and physiological temperature (22 °C and 36 °C). If the length of this pulse was found to be insufficient for the drug to reach equilibrium within the first pulse, the experiments were repeated with a 40 s depolarizing pulse. This latter strategy was necessary for 100 nM bepridil, 30 nM cisapride, 100 nM terfenadine, and 100 nM dofetilide at ambient temperature. The measured timecourse of onset of drug block ( $\tau_{on}$ ) was both drug and concentration dependent (Figure 1A, Table 1) in agreement with our previous study using the gold standard manual patch-clamp technique (Windley et al., 2017). Furthermore, all of the drugs tested displayed temperature dependent kinetics, with  $\tau_{on}$  significantly faster at physiological temperature (Figure 1B). On the other hand, the degree of block was found to be relatively insensitive to changes in temperature (Supplementary Figure 1B).

While  $\tau_{on}$  was temperature dependent for all the drugs tested, the degree of temperature dependence of  $\tau_{on}$  was different for each individual drug. For example, 100 nM bepridil exhibited a decrease in  $\tau_{on}$  of 2.0-fold, while 100 nM cisapride showed a decrease of 4.2-fold between ambient and physiological temperatures.  $\tau_{on}$  for diltiazem could not be accurately measured at 36°C as the timecourse of block was equivalent or faster than the onset of current, resulting in an apparent instantaneous block, as described previously by Windley et al., 2017 for ambient temperature recordings.

MOL #111534

## Drug trapping

Since the degree of drug trapping has also been flagged as a potentially important determinant of AP prolongation and a potential marker for proarrhythmic risk (Colatsky et al., 2016; Di Veroli et al., 2014; Li et al., 2017), the temperature dependence of trapping characteristics for each of the drugs was also measured. Diltiazem was excluded from this analysis as the kinetics of block were too rapid to measure. The degree of trapping was determined by measuring the percentage block at the onset of the final 0 mV sweep in the presence of drug (estimated by extrapolation of a fitted curve back to the beginning of the current onset ( $t = 0$ )), normalized against the degree of block at the end of the sweep as previously described (Figure 2A) (Windley et al., 2017). In general, temperature had little effect on the degree of trapping (Figure 2C). For verapamil, there was no significant trapping at either temperature:  $1.1 \pm 1.1\%$  at  $22^\circ\text{C}$  and  $1.7 \pm 1.7\%$  at  $36^\circ\text{C}$ . Similarly, for dofetilide and bepridil apparent trapping at ambient temperature was not significantly different to that observed at physiological temperature. Cisapride, on the other hand, exhibited significantly less trapping at physiological than at ambient temperature ( $45.6 \pm 4.8\%$  and  $66.1 \pm 4.0\%$  respectively at 30 nM), while terfenadine exhibited an increased degree of trapping at the higher temperature ( $87.0 \pm 2.7$  compared to  $99.7 \pm 0.3\%$ ). In the latter case, the lower degree of trapping at ambient temperature is likely an artifact of the significant noise exhibited in the first 1-2 s of the subtracted trace. This noise is a result of the slower current onset, an issue which is somewhat eliminated at higher temperatures where the channel activation is much faster (Vandenberg et al., 2006). For cisapride however, we hypothesized that the reduction in apparent trapping at physiological temperature could be explained by the fact



MOL #111534

that cisapride is not truly trapped, but merely dissociates slowly and that at physiological temperature, additional drug washout occurs during the interpulse interval because the timecourse of dissociation is accelerated by increased temperature. To test this hypothesis we assessed the impact of altering the interpulse interval between successive depolarizing pulses at ambient temperature (Figure 2B) using manual patch-clamp. In these experiments, the response for cisapride was compared to that of bepridil, a drug that had no significant relief of trapping at physiological temperature, yet has a similar timecourse of drug washout as assessed using a separate protocol (Supplementary Figure 2B). The apparent degree trapping of cisapride was significantly reduced with longer interpulse intervals ( $68.7 \pm 4.6\%$  and  $30.5 \pm 5.1\%$  trapped with 10 s and 60 s interpulse respectively) which is consistent with the measured  $\tau_{\text{off}}$  of  $\sim 45$  s (Supplementary Figure 2B, Windley et al., 2016), while the response of bepridil remained unchanged (Figure 2D).

### Temperature dependence of association and dissociation rates

To probe the temperature dependence of kinetics in more detail we assumed a bimolecular model of drug binding (see scheme 1, eqn 3 and 4) to allow us to calculate approximations of the rates of association ( $k_{\text{on}}$ ) and dissociation ( $k_{\text{off}}$ ) for drug binding to hERG (Table 2). This model assumes that binding is equivalent to open and inactive states of the channel and that binding is a simple diffusion limited process (see Scheme 1). This is likely an overly simplified model for two reasons. First, using a different protocol that allowed direct measurement of the rates of binding and unbinding, we have shown that the kinetics of binding of clozapine to the open and inactive states of hERG are different (Hill *et al.* 2014). Second, we have shown that for cisapride, first order kinetics do not hold, but rather a

MOL #111534

multistep binding reaction, including an encounter complex, is necessary to describe binding to hERG, particularly at physiological temperatures (Windley et al., 2016). However, in the specific context of the CiPA protocol being examined here, this is a useful, albeit simple model since it provides a framework for us to interrogate the influence of temperature dependent drug binding kinetics on modelled cardiac APs. Furthermore, both of the assumptions - the bimolecular formulation and equivalent binding to open versus inactivated states - is consistent with the approach currently being employed as part of CiPA (Dutta et al., 2017; Li et al., 2017; Li et al., 2016). Under these assumptions, and by considering the timecourse of block ( $\tau_{on}$ , Figure 3A, Table 1) for two drug concentrations, the timecourse of drug washout ( $\tau_{off}$ , Figure 3B, Table 2), as well as  $k_{on}$  (Figure 3C, Table 2) and  $k_{off}$  (Figure 3D, Table 2) were calculated. Increasing temperature increased both  $k_{on}$  and  $k_{off}$  for four drugs (verapamil, cisapride, bepridil and terfenadine). The temperature dependence of these effects varied for the different drugs (Figure 3, Table 2). Specifically, for  $k_{on}$ , the magnitude of the temperature dependent increase in rate between ambient and physiological temperatures ranged from 2.4-fold (for verapamil) to 7-fold (for cisapride), corresponding to calculated  $Q_{10}$  values of 1.7 and 5 respectively. On the other hand, the calculated changes in  $\tau_{off}$ , and hence  $k_{off}$ , were most substantial for verapamil with a  $Q_{10}$  of 3.9 in comparison to bepridil with a  $Q_{10}$  of 1.0.

### **Impact of temperature dependent drug block kinetics on action potential repolarization**

To examine the physiological impact of the range of association and dissociation rates observed as a function of temperature, we incorporated a kinetic scheme for the hERG/drug interaction, including calculated values for  $k_{on}$  and  $k_{off}$ , into the O'Hara-Rudy model of the

MOL #111534

ventricular AP (O'Hara et al., 2011) (see Materials and Methods) and the degree of AP prolongation at 1 Hz pacing was measured for each of the drugs (Figure 4). Cisapride, bepridil and terfenadine resulted in more prolonged AP durations (APD) when simulated with kinetics data derived at physiological temperature in comparison to ambient temperature (Table 3, Figure 5B, 44, 34 and 129 ms prolongation for 30nM cisapride, 100nM bepridil, and 10nM and terfenadine respectively), while verapamil block resulted in less prolongation at physiological temperature (50 ms shortening of APD at 100nM) (Figure 5B). The responses for terfenadine were simulated with 10 nM [drug] as both 100 and 1  $\mu$ M resulted in EADs due to almost complete block of  $I_{Kr}$  (data not shown).

We next evaluated whether it might be feasible to apply a common scaling factor to rates derived from ambient temperature data in order to extrapolate to physiological temperature (Figure 5), since this has been proposed as a potential approach for CiPA and would represent a simpler approach for industry implementation. Given the changes in calculated  $k_{on}$  and  $k_{off}$  for the panel of drugs studied here varied between  $\sim$ 2- and  $\sim$ 7-fold in response to the change from ambient to physiological temperature (Figure 3), we implemented a number of different theoretical scenarios *in silico* based on these bounds. In the scenario where changes in  $k_{on}$  and  $k_{off}$  of equal magnitude (either 2 fold or 7 fold) were implemented, very little, if any further prolongation was observed for each of the drugs (data not shown). However, varying  $k_{on}$  and  $k_{off}$  to different degrees resulted in significant changes in APD prolongation for all four of the drugs (Figure 5A and B). While increasing  $k_{on}$  by 7-fold and  $k_{off}$  by only 2-fold resulted in a significant prolongation (eg. 30 nM cisapride APD<sub>90</sub> was 427 ms), the converse rate alterations actually resulted in AP shortening (eg. 30 nM cisapride APD<sub>90</sub> was 343 ms, Figure 5A and B). The change in APD<sub>90</sub> was closely related to the degree

MOL #111534

of  $I_{Kr}$  block seen, such that faster  $k_{on}$  relative to  $k_{off}$  values resulted in more block of  $I_{Kr}$  and AP prolongation while the converse was true for AP shortening (data not shown).

MOL #111534

## Discussion

In this study, we present the first detailed analysis of the temperature dependence of hERG drug block kinetics, measured using the CiPA step depolarization protocol (Windley et al., 2017). This is a critical question that will determine at which temperature *in vitro* data needs to be acquired to constrain *in silico* models for risk prediction. We show that for a range of drugs, the kinetics of block are substantially different at physiological compared to ambient temperature and demonstrate using *in silico* simulations that this difference in kinetics translates to variable effects on action potential prolongation for equivalent concentrations of drug. Furthermore, individual drugs showed different temperature dependencies of block kinetics. As a result, extrapolating from data acquired at ambient temperature to make a reasonable inference of physiological temperature rates is not possible. Therefore, if physiological temperature models of the kinetics of drug binding need to be accurately constrained for *in silico* proarrhythmic risk prediction, the *in vitro* data should be acquired at physiological temperature. In the context of the current standard, where most data acquired in preclinical screening is gathered on automated electrophysiological platforms that operate at ambient temperature, this is a significant issue for the field in terms of gathering data for *in silico* risk prediction.

### Temperature dependence of drug binding kinetics

Using the CiPA step depolarization protocol, designed to interrogate potency and kinetics of drug block on HT patch-clamp platforms, we examined the temperature dependence of six hERG blocking drugs. While the measured potency of block was only subtly, if at all, affected by temperature, the observed onset of block ( $\tau_{on}$ ) was significantly faster at physiological

MOL #111534

temperature for all drugs. To approximate the temperature dependence of individual binding ( $k_{on}$ ) and unbinding rates ( $k_{off}$ ), the timecourse of onset of block was measured for two concentrations of each drug at both ambient (22°C) and physiological temperature (36°C), and  $k_{on}$  and  $k_{off}$  derived by simultaneous solution, assuming a simple bimolecular interaction. This assumption was made because i) Given the nature of the datasets acquired using this protocol, it would be unrealistic to parameterize a more complex model; and ii) This assumption is relevant to the model structure being implemented as part of CiPA (Dutta et al., 2017; Li et al., 2017; Li et al., 2016). In all cases,  $k_{on}$  and  $k_{off}$  were increased at physiological temperature, but to varying degrees between 2 and 7 fold. In most cases  $k_{on}$  was found to be more temperature dependent than  $k_{off}$ , with the exception of verapamil with relatively less temperature sensitivity for  $k_{on}$  and larger sensitivity for  $k_{off}$ . Whilst we are cautious in attaching concrete interpretation to these rates from the simple model we have used, it is interesting to consider why this might be the case. CHO cells constitutively express P-glycoprotein (PGP) (Bresden *et al.* 1994), a transporter that facilitates movement of drugs across biological membranes. The temperature sensitivity of drug binding rates observed in this type of assay could therefore be a combination of the effect of temperature directly on the drug/channel interaction as well as on the biological activity of PGP in setting the equilibrium concentration of drug in the cytosolic compartment. Verapamil inhibits PGP, which could contribute to the observed difference in the temperature sensitivity of rates compared to the other drugs tested. This also has potential implications for assays in different heterologous systems (CHO versus HEK cells for example) that express different levels of PGP and perhaps highlights a further important role for assays in cardiomyocytes (where PGP expression is absent or very low under basal conditions (Meissner *et al.* 2002,

MOL #111534

Cordon-Cardo *et al.* 1990)), to ensure that potencies and drug binding rates are measured in a physiologically appropriate context.

### ***In silico* assessment of the significance of temperature dependent kinetics**

To assess the significance of these temperature dependent kinetics on cardiac repolarization, the calculated rates were incorporated into the O'Hara-Rudy *in silico* model of the cardiac AP (O'Hara et al., 2011). Cisapride, bepridil and terfenadine all showed greater prolongation of the AP when physiological temperature rates were used compared to ambient temperature. Conversely, verapamil shortened the AP in simulations using physiological temperature rates in comparison to those using ambient temperature rates (Table 3) as a consequence of the greater temperature dependence of  $k_{off}$  versus  $k_{on}$  for verapamil.

### **Can physiological temperature kinetics be extrapolated from ambient temperature data?**

Our analysis shows that drug binding kinetics estimated from data gathered at different temperatures significantly affect the degree of repolarization prolongation assessed *in silico*. This observation has important implications for how *in vitro* data, that is to be used to constrain models for assessment of proarrhythmic risk *in silico*, should be gathered. For many automated electrophysiological platforms acquisition at physiological temperature is not an option. An alternative is that all kinetic data be gathered using manual patch clamp - the approach that was employed in development of the current CiPA models by the *in silico*

MOL #111534

working group (Dutta et al., 2017; Li et al., 2017). However, this is not a viable option for industry, where a requirement for high throughput is central to any screening approach.

An alternative might be that a single set of scaling factors, derived from experiments on a range of existing drugs, could be used to extrapolate ambient temperature rates to physiological temperature. We evaluated a range of scaling factors, covering the minimum and maximum  $Q_{10}$  values obtained for both  $k_{on}$  and  $k_{off}$  for the four drugs in this study. Our data show that none of the scalars applied can account for the temperature dependence in more than one drug. Given this complication, a feasible approach that would incorporate some 'safety buffer' might be to use the scalar set that results in the most severe effects on AP prolongation. However, this is likely to result in incorrect classification of some safe drugs as dangerous – exactly the problem that exists with current preclinical screening that CiPA aims to remedy (Fermini et al., 2016; Sager et al., 2014). Perhaps a more nuanced approach might be identification of subclasses of compounds for which different sets of scalars could be used. Some of the seminal work on the structural basis for aLQTS showed how different drugs differentially interact with residues in the hERG pore as demonstrated by mutation of the key drug binding residues (Mitcheson *et al.* 2000). One could envisage that compounds that share modes of binding might also share features of their temperature dependence, meaning common scaling factors could be used. However, such an approach would be dependent on acquisition of temperature dependence data from a larger and more diverse panel of drugs on both WT and mutant channels to identify potential subclasses and assess whether subclasses share common temperature sensitivities. It should also be considered that any conclusions in regard to use of scaling factors is made in the context of the likely variability in the kinetic data collected across different HT platforms. For example, a



MOL #111534

previously published comparison of potency for a range of drugs on different HT platforms showed that measured  $IC_{50}$  values can differ by as much as an order of magnitude (Mirams et al., 2014). While it remains to be seen whether this will be a similar issue for kinetic measurements (the CiPA HT stream is currently working to answer this question), it is more than likely to be the case. Therefore, any possible over-classification of risk associated with using temperature scale factors should be considered relative to this probable degree of error. Furthermore, in light of the practicalities of performing the experiments at physiological temperatures which is not possible on many systems, and even where possible is practically a more difficult approach which may limit the throughput of screening, the use of scalars to extrapolate between temperatures may be an acceptable 'good enough' solution.

### **Drug trapping**

Drug trapping has been identified as a potentially important parameter in the assessment of proarrhythmic risk *in silico* (Colatsky et al., 2016; Di Veroli et al., 2014; Li et al., 2017). In this study, the degree of trapping measured using the step depolarization protocol was consistent with existing literature. Specifically, verapamil did not undergo trapping, terfenadine and dofetilide were completely trapped, while bepridil displayed an intermediate level of trapping (Li et al., 2017; Stork et al., 2007; Zhang et al., 1999). For most drugs, the degree of trapping was independent of temperature. However, for cisapride, the degree of trapping was reduced at physiological temperature. We hypothesized that the

MOL #111534

'virtual' trapping of cisapride measured using this protocol may be a function of slow dissociation of the drug relative to the 15 second hyperpolarized interpulse interval over which trapping is assayed, rather than true trapping, where the drug is locked in the channel pore by a closed cytoplasmic gate. Under this scenario, at higher temperatures where the  $k_{off}$  is faster, less 'virtual' trapping is evident as more of the drug population dissociates during the interpulse interval. To test this, we assayed trapping with two variations of the step depolarization protocol with different periods of channel closure (10 s and 60 s). Consistent with our hypothesis, cisapride appeared more trapped with shorter interpulse intervals and less trapped with longer intervals. Furthermore, the degree of trapping observed for the 10 and 60 s intervals (68.7 and 30.5 % respectively) was consistent with the measured  $\tau_{off}$  of ~46 s for cisapride that measured using a different protocol (Windley et al., 2016). Conversely, for bepridil, a drug which displays true trapping, the degree of trapping is not affected by temperature, even though bepridil and cisapride have similar  $\tau_{off}$  values (Supplementary Figure 2B). Existing literature suggests that trapped drugs cause more prolongations than slow dissociating drugs (Di Veroli et al., 2014). Given our data, cisapride falls into the latter of these categories, while bepridil falls into the former, yet they are indistinguishable using the step depolarization protocol at ambient temperature. While current CiPA-led efforts to assign risk *in silico* based on data derived from this protocol look extremely promising (Li et al., 2017), they lump both virtual and truly trapped drugs together. Future efforts to refine these models, and further improve their ability to stratify risk might necessitate efforts to distinguish drugs that display virtual as opposed to true trapping, as well as state dependent binding.

MOL #111534

## Limitations

The *in vitro* data in this study is all measured from a CHO cell line stably expressing the hERG-1a isoform, whereas native  $I_{Kr}$  is carried by heteromeric hERG 1a/1b and associated accessory proteins. The potency of many drugs has been shown to be different for hERG 1a versus 1a/1b complexes (Abi-Gerges *et al.* 2011), and this is likely to extend to drug binding kinetics, meaning these factors should be considered in assessing the physiological implications of this study.

## Conclusions

Here we present the first detailed analysis of the temperature dependence of kinetics and trapping for drug block of hERG channels, measured using the CiPA step depolarization protocol (Windley *et al.*, 2017). In all cases, the observed onset of block was significantly faster at physiological temperature, with calculated association and dissociation rates showing  $Q_{10}$  values varying between 1 and 5 - with each drug having different temperature dependencies. This spectrum of temperature dependent rates resulted in variable effects on repolarization for different drugs ranging between either AP prolongation or AP shortening when kinetic rate constants for physiological temperature versus those acquired at ambient

MOL #111534

temperature were included in *in silico* models of ventricular electrophysiology. Because of these drug specific effects, a single set of scaling factors could not describe the temperature dependence of kinetics for any more than one drug. This indicates that the temperature at which drug kinetic information is acquired is crucial to the accurate prediction of proarrhythmic risk *in silico*. Accordingly, if physiological temperature models of the kinetics of drug binding need to be accurately constrained for *in silico* proarrhythmic risk prediction, the *in vitro* data should be acquired at physiological temperature.

MOL #111534

## **Acknowledgements**

The authors thank Dr Matthew Perry, Mark Hunter, Dr Bernard Fermini, Dr Jules C. Hancox and Dr Najah Abi-Gerges for informative discussion.

MOL #111534

## **Authorship Contributions**

Participated in research design: Windley, Hill, Lee, Vandenberg

Conducted experiments: Windley

Contributed to new reagents or analytical tools: Hill, Vandenberg

Performed data analysis: Windley, Lee, Hill

Wrote or contributed to the writing of the manuscript: Windley, Hill, Lee, Vandenberg

MOL #111534

## References

- Abi-Gerges, N., Holkham, H., Jones, E. M. C., Pollard, C. E., Valentin, J. P., & Robertson, G. A. (2011). hERG subunit composition determines differential drug sensitivity. *British Journal of Pharmacology*, *164*(2b), 419–432
- Aiba T, Shimizu W, Inagaki M, Noda T, Miyoshi S, Ding WG, Zankov DP, Toyoda F, Matsuura H, Horie M and Sunagawa K (2005) Cellular and ionic mechanism for drug-induced long QT syndrome and effectiveness of verapamil. *JACC* **45**(2): 300-307.
- Barry PH (1994) JPCalc, a software package for calculating liquid junction potential corrections in patch-clamp, intracellular, epithelial and bilayer measurements and for correcting junction potential measurements. *Journal of neuroscience methods* **51**(1): 107-116.
- Brezden, C. B., Hedley, D. W., & Rauth, A. M. (1994). Constitutive expression of P-glycoprotein as a determinant of loading with fluorescent calcium probes. *Cytometry*, *17*(4), 343–348.
- Colatsky T, Fermini B, Gintant G, Pierson JB, Sager P, Sekino Y, Strauss DG and Stockbridge N (2016) The Comprehensive in Vitro Proarrhythmia Assay (CiPA) initiative - Update on progress. *Journal of pharmacological and toxicological methods* **81**: 15-20.
- Cordon-Cardo, C., O'Brien, J. P., Boccia, J., Casals, D., Bertino, J. R., & Melamed, M. R. (1990). Expression of the multidrug resistance gene product (P-glycoprotein) in human normal and tumor tissues. *The Journal of Histochemistry and Cytochemistry : Official Journal of the Histochemistry Society*, *38*(9), 1277–1287.
- Crumb WJ, Jr., Vicente J, Johannesen L and Strauss DG (2016) An evaluation of 30 clinical drugs against the comprehensive in vitro proarrhythmia assay (CiPA) proposed ion channel panel. *Journal of pharmacological and toxicological methods* **81**: 251-262.

MOL #111534

- Di Veroli GY, Davies MR, Zhang H, Abi-Gerges N and Boyett MR (2014) hERG inhibitors with similar potency but different binding kinetics do not pose the same proarrhythmic risk: implications for drug safety assessment. *Journal of cardiovascular electrophysiology* **25**(2): 197-207.
- Dutta S, Chang KC, Beattie KA, Sheng J, Tran PN, Wu WW, Wu M, Strauss DG, Colatsky T and Li Z (2017) Optimization of an in silico cardiac cell model for proarrhythmia risk assessment. *Frontiers in physiology* **8**: 616.
- Fermini B, Hancox JC, Abi-Gerges N, Bridgland-Taylor M, Chaudhary KW, Colatsky T, Correll K, Crumb W, Damiano B, Erdemli G, Gintant G, Imredy J, Koerner J, Kramer J, Levesque P, Li Z, Lindqvist A, Obejero-Paz CA, Rampe D, Sawada K, Strauss DG and Vandenberg JI (2016) A new perspective in the field of cardiac safety testing through the comprehensive in vitro proarrhythmia assay paradigm. *Journal of biomolecular screening* **21**(1): 1-11.
- Food and Drug Administration H (2005) International Conference on Harmonisation; guidance on S7B Nonclinical Evaluation of the Potential for Delayed Ventricular Repolarization (QT Interval Prolongation). *Federal Register* **70**(1): 10.
- Hill, A. P., Perrin, M. J., Heide, J., Campbell, T. J., Mann, S. A., & Vandenberg, J. I. (2014). Kinetics of drug interaction with the Kv11.1 potassium channel. *Molecular Pharmacology*, *85*(5), 769–776.
- Lee W, Mann SA, Windley MJ, Imtiaz MS, Vandenberg JI and Hill AP (2016) In silico assessment of kinetics and state dependent binding properties of drugs causing acquired LQTS *Progress in biophysics and molecular biology* **120**(1-3): 89-99.



MOL #111534

Li Z, Dutta S, Sheng J, Tran PN, Wu W, Chang K, Mdluli T, Strauss DG and Colatsky T (2017)

Improving the in silico assessment of proarrhythmia risk by combining hERG (Human Ether-a-go-go-Related Gene) channel-drug binding kinetics and multichannel pharmacology. *Circ Arrhythm Electrophysiol* **10**(2): e004628.

Li Z, Dutta S, Sheng J, Tran PN, Wu W and Colatsky T (2016) A temperature-dependent in silico model of the human ether-a-go-go-related (hERG) gene channel. *Journal of pharmacological and toxicological methods* **81**: 233-239.

Lu Y, Mahaut-Smith MP, Varghese A, Huang CL, Kemp PR and Vandenberg JI (2001) Effects of premature stimulation on HERG K(+) channels. *The Journal of physiology* **537**(Pt 3): 843-851.

Martin RL, McDermott JS, Salmen HJ, Palmatier J, Cox BF and Gintant GA (2004) The utility of hERG and repolarization assays in evaluating delayed cardiac repolarization: influence of multi-channel block. *Journal of cardiovascular pharmacology* **43**(3): 369-379.

Meissner, K., Sperker, B., Karsten, C., Meyer Zu Schwabedissen, H., Seeland, U., Böhm, M., et al. (2002). Expression and localization of P-glycoprotein in human heart: effects of cardiomyopathy. *The Journal of Histochemistry and Cytochemistry : Official Journal of the Histochemistry Society*, *50*(10), 1351–1356.

Mirams GR, Davies MR, Brough SJ, Bridgland-Taylor MH, Cui Y, Gavaghan DJ and Abi-Gerges N (2014) Prediction of Thorough QT study results using action potential simulations based on ion channel screens. *Journal of pharmacological and toxicological methods* **70**(3): 246-254.

MOL #111534

- Mitcheson, J. S., Chen, J., Lin, M., Culberson, C., & Sanguinetti, M. C. (2000). A structural basis for drug-induced long QT syndrome. *Proceedings of the National Academy of Sciences of the United States of America*, 97(22), 12329–12333.
- O'Hara T, Virag L, Varro A and Rudy Y (2011) Simulation of the undiseased human cardiac ventricular action potential: model formulation and experimental validation. *PLoS computational biology* 7(5): e1002061.
- Redfern WS, Carlsson L, Davis AS, Lynch WG, MacKenzie I, Palethorpe S, Siegl PK, Strang I, Sullivan AT, Wallis R, Camm AJ and Hammond TG (2003) Relationships between preclinical cardiac electrophysiology, clinical QT interval prolongation and torsade de pointes for a broad range of drugs: evidence for a provisional safety margin in drug development. *Cardiovascular research* 58(1): 32-45.
- Sager PT, Gintant G, Turner JR, Pettit S and Stockbridge N (2014) Rechanneling the cardiac proarrhythmia safety paradigm: a meeting report from the Cardiac Safety Research Consortium. *Am Heart J* 167(3): 292-300.
- Shah RR (2008) Drug-induced QT interval prolongation—regulatory guidance and perspectives on hERG channel studies, in *The hERG cardiac potassium channel: structure, function and long QT syndrome* pp 251-285, John Wiley & Sons, Ltd.
- Stork D, Timin EN, Berjukow S, Huber C, Hohaus A, Auer M and Hering S (2007) State dependent dissociation of HERG channel inhibitors. *British journal of pharmacology* 151(8): 1368-1376.
- Walker BD, Singleton CB, Bursill JA, Wyse KR, Valenzuela SM, Qiu MR, Breit SN and Campbell TJ (1999) Inhibition of the human ether-a-go-go-related gene (HERG)

MOL #111534

potassium channel by cisapride: affinity for open and inactivated states. *British journal of pharmacology* **128**(2): 444-450.

Windley MJ, Abi-Gerges N, Fermini B, Hancox JC, Vandenberg JI and Hill AP (2017)

Measuring kinetics and potency of hERG block for CiPA. *Journal of pharmacological and toxicological methods* **87**: 99-107.

Windley MJ, Mann SA, Vandenberg JI and Hill AP (2016) Temperature effects on kinetics of

KV11.1 drug block have important consequences for in silico proarrhythmic risk prediction. *Molecular pharmacology* **90**(1): 1-11.

Yap YG and Camm AJ (2003) Drug induced QT prolongation and torsades de pointes. *Heart*

**89**(11): 1363-1372.

Zhang S, Zhou Z, Gong Q, Makielski JC and January CT (1999) Mechanism of block and

identification of the verapamil binding domain to HERG potassium channels. *Circulation research* **84**(9): 989-998.

MOL #111534

## Footnotes

This work was supported by grants from the National Health and Medical Research Council of Australia [APP1088214]. JIV is supported by an NHMRC Senior Research Fellowship [APP1019693]. WL is supported by a National Heart Foundation of Australia Health Professional Scholarship [APP101552].

MOL #111534

## Legends for Figures

**Figure 1.** *Temperature dependence of hERG drug block onset.* **A.** The timecourse of drug block was measured using the depicted offline subtraction routine, where the first 0 mV trace in the presence of drug was subtracted from the control hERG current. The resultant trace (black line) was then fit with a single component exponential function (grey broken line) to give a time constant value for the onset of block,  $\tau_{on}$ . **B.** Data points represent  $\tau_{on}$  values for each of the six drugs. At each concentration of drug the  $\tau_{on}$  values obtained at 22 (closed circle) and 36°C (open square) were compared and the fold change values listed above, all comparisons were statistically significant ( $p < 0.05$ , Mann Whitney's non-parametric test). Each data point represents the mean  $\pm$  SE for  $n = 4-6$  cells. The subtracted data obtained from 30  $\mu$ M diltiazem at 36°C could not be adequately fit with an exponential function, therefore no data was recorded and this is designated by an asterisk.

**Figure 2.** *The temperature dependence of drug trapping.* **A.** To measure drug trapping the first (black) and last (red) current trace recorded in the presence of drug was subtracted from the control current and the resultant traces fit with an exponential function. The traces were extrapolated back to time = 0 and the degree of block measured at the beginning of the final drug trace (I) was calculated as a percentage of the level of steady state block (II) to give the percentage of trapped drug. **B.** To assess the influence of the interpulse interval on the measured degree of drug trapping consecutive 0 mV pulses from a holding potential of -80 mV were applied with 10, 15 or 60 s interpulse intervals. **C.** Drug trapping measurements were taken from data collected at 22 (closed circles) and 36°C (open squares) in response to 1-2 concentrations of each drug. Trapping was measured with an interpulse interval of 15 s.

MOL #111534

Each data point represents the mean  $\pm$  SE of  $n = 4-6$  cells. The temperature dependence of trapping was assessed for each drug and concentration by comparing data collected at 22 and 36°C ( $p < 0.05$ , non-parametric Mann Whitney test), statistically significant responses are designated with an asterisks. **D**. The degree of trapping was assessed for two drugs, cisapride (yellow) and bepridil (blue) in response to 0 mV pulse protocols containing 10 (closed circle) or 60 s (open square) interpulse intervals. The degree of trapping measured for cisapride using a 10 or 60 s interpulse interval was significantly different while bepridil responses were not. Statistically significant responses are designated with an asterisk ( $p < 0.05$ , non-parametric Mann Whitney's test). Each data point represents the mean  $\pm$  SE of  $n = 4-6$  cells.

**Figure 3.** *Temperature dependence of drug block timecourse and rate constants.* Plots represent the measured time constants for onset of block (**A**,  $\tau_{on}$ ), the calculated time constants for drug washout ( $k_{off}$ , **B**), the calculated rate of drug binding ( $k_{on}$ , **C**) and the calculated rate of drug dissociation ( $k_{off}$ , **D**). The values for plots B-D were calculated from the experimentally measured  $\tau_{on}$  values with a minimum of two concentrations per drug using a simple bi-molecular model of drug block. Only the values from plot A represent the mean  $\pm$  SE of 4-6 cells, while the remaining plots were obtained using averaged  $\tau_{on}$  values from plot A. Values for each plot were compared at 22 (closed circles) and 36°C (open squares) and the fold change (A-B) or Q10 (C-D) values are shown above the relevant data points.

MOL #111534

**Figure 4.** *Examining the impact of temperature dependent drug kinetics on modeled cardiac action potentials at 1 Hz.* Modelled traces representing simulations of the  $I_{Kr}$  (i) or the cardiac action potential (ii) based on the ORD11 model for 300 nM verapamil (A), 30 nM cisapride (B), 100 nM bepridil (C) and 10 nM terfenadine (D). The blue traces represent control or drug-free simulations while the orange and green traces represent traces simulated using the drug kinetics calculated from 22 and 36°C data, respectively.

**Figure 5.** *Modeling the implementation of a scalar of block kinetics at 22°C to predict proarrhythmic risk.* (A) A number of scalars based on the range of temperature dependent changes to the binding kinetics were applied to data collected at 22°C to determine if it was possible to predict the change in kinetics seen at 36°C. Change in APD<sub>90</sub> was examined for 300 nM verapamil (red circle), 30 nM cisapride (yellow square), 100 nM bepridil (blue triangle) and 10 nM terfenadine (purple diamond). The AP<sub>90</sub> for control APs is represented by a dotted line. (B) Change in APD<sub>90</sub> when compared to rates derived from data recorded at 22°C. ΔAPD<sub>90</sub> represents the difference in simulated APD<sub>90</sub> values when rates of drug block are scaled (red and grey) or measured at 36°C (black) and are compared for each drug.

MOL #111534

## Tables

**Table 1:** *Temperature dependence of drug block onset.*

The timecourse of block onset ( $\tau_{on}$ ) was measured at 22 and 36°C by fitting an exponential function to drug block data.

	$\tau_{on}$ (s)					
	22°C				36°C	
	Conc. 1	Conc. 2	Conc. 1	Conc. 2	Conc. 1	Conc. 2
<b>verapamil</b>	100	300	5.30	2.97	1.24	0.86
<b>cisapride</b>	30	100	10.96	5.95	2.59	1.08
<b>bepriidil</b>	100	1000	3.20	0.67	1.58	0.25
<b>terfenadine</b>	100	1000	10.82	1.13	2.07	0.21
<b>dofetilide</b>	100	-	30.30	-	7.43	-
<b>diltiazem</b>	30	-	0.84	-	-	-



MOL #111534

**Table 2:** *Temperature dependence of drug block rates.*

The calculated timecourse of drug washout ( $\tau_{off}$ ), rate of drug binding ( $k_{on}$ ) and rate of drug dissociation ( $k_{off}$ ) at 22 and 36°C were derived using a simple bimolecular model of hERG drug binding.

	$\tau_{off}$ (s)		$k_{on}$ ( $M^{-1}\cdot s^{-1}$ )		$k_{off}$ ( $s^{-1}$ )	
	22°C	36°C	22°C	36°C	22°C	36°C
<b>verapamil</b>	8.89	1.60	$7.51 \times 10^5$	0.113	$1.78 \times 10^6$	0.626
<b>cisapride</b>	17.15	6.46	$1.10 \times 10^6$	0.058	$7.71 \times 10^6$	0.155
<b>bepriidil</b>	5.52	3.86	$1.32 \times 10^6$	0.181	$3.74 \times 10^6$	0.259
<b>terfenadine</b>	217.39	116.28	$8.80 \times 10^5$	0.005	$4.73 \times 10^6$	0.009

MOL #111534

**Table 3:** *Change in APD<sub>90</sub> in response to varying drug kinetics of block.*

AP simulations were run with rates calculated from 22 and 36°C experimental data or with scalars applied to 22°C calculated rates. The change in APD<sub>90</sub> is expressed as the difference between AP data in the presence and absence of drug under the listed conditions.

		<b>ΔAPD<sub>90</sub> (ms)</b>					
		<b>22°C</b>	<b>36°C</b>	<b>x2 k<sub>on</sub>, k<sub>off</sub></b>	<b>x7 k<sub>on</sub>, k<sub>off</sub></b>	<b>x2 k<sub>on</sub>, x7 k<sub>off</sub></b>	<b>x7 k<sub>on</sub>, x2 k<sub>off</sub></b>
<b>300 nM</b>							
<b>verapamil</b>		44	-6	45	55	-20	196
<b>30nM</b>							
<b>cisapride</b>		29	73	29	29	8	92
<b>100 nM</b>							
<b>bepidil</b>		37	71	38	43	12	121
<b>10 nM</b>							
<b>terfenadine</b>		75	204	87	89	28	234

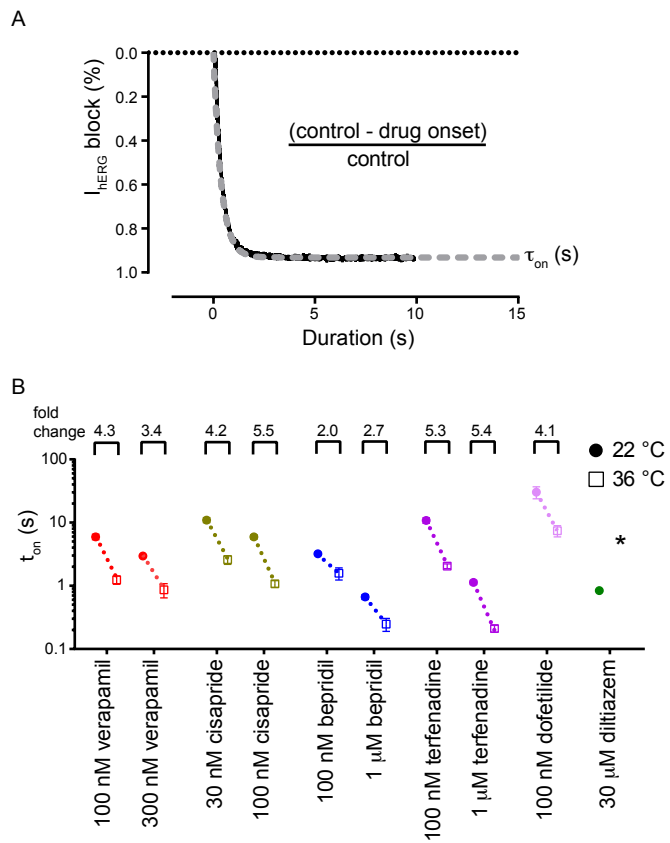


Figure 1

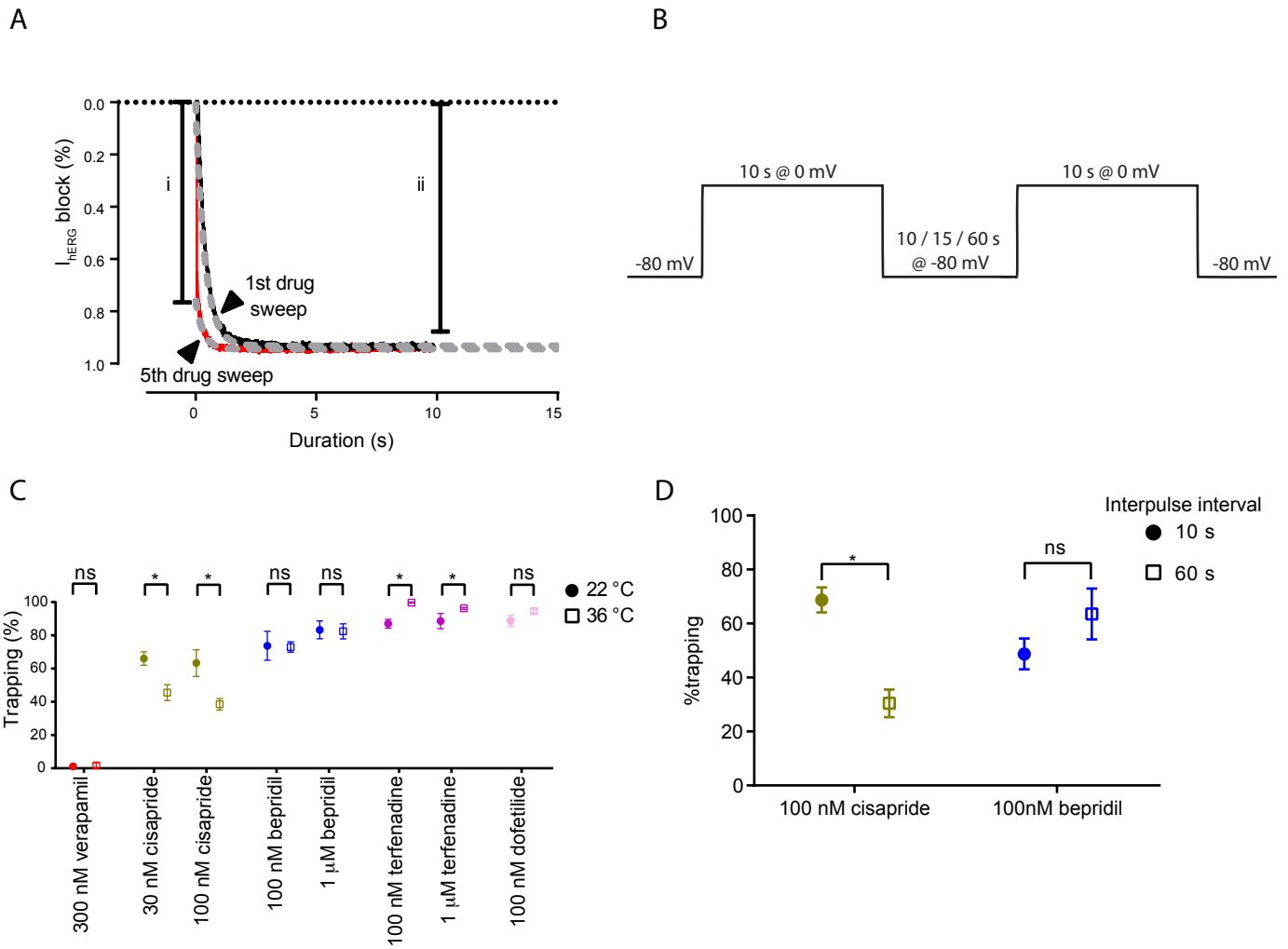


Figure 2

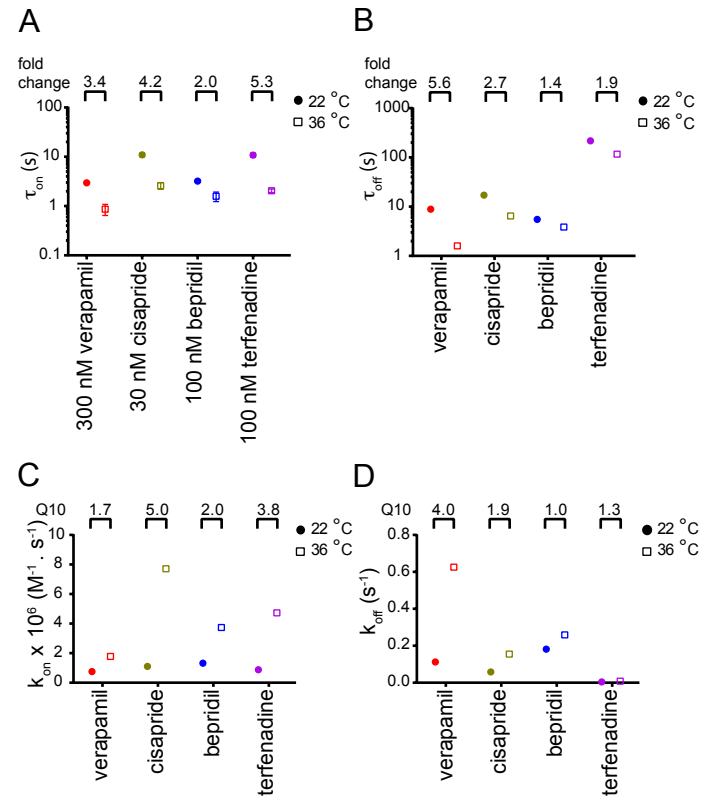


Figure 3

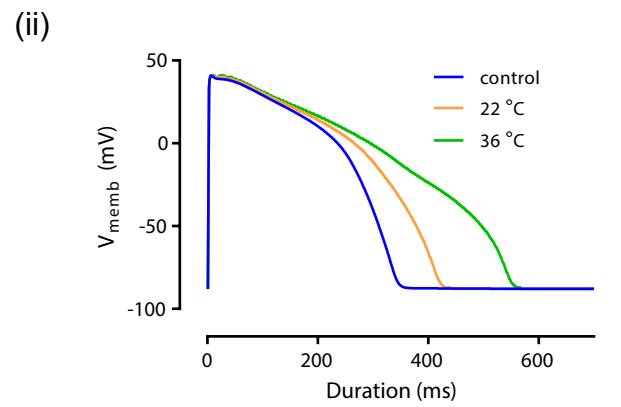
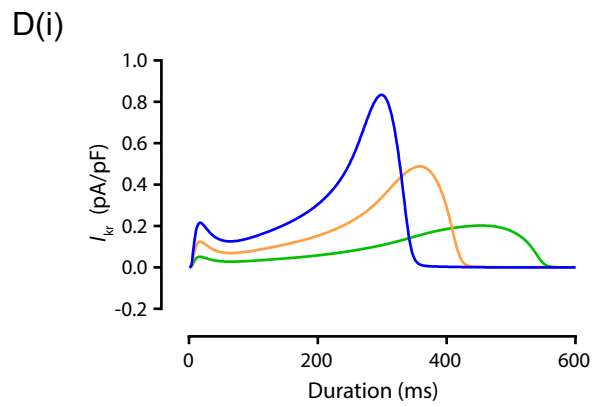
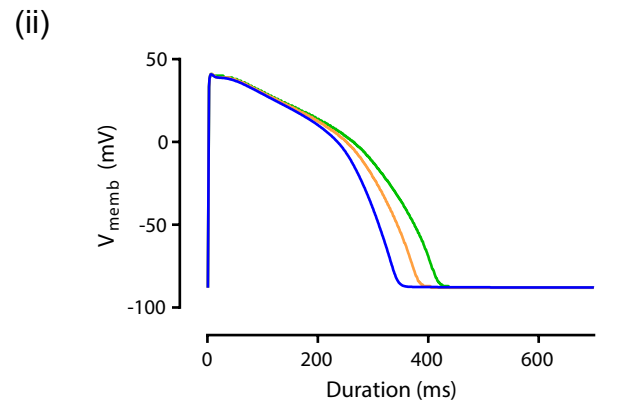
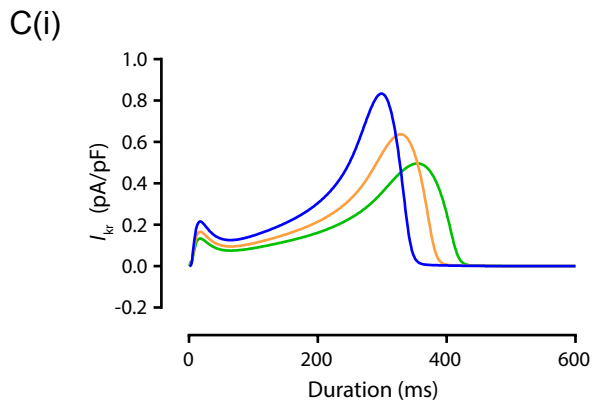
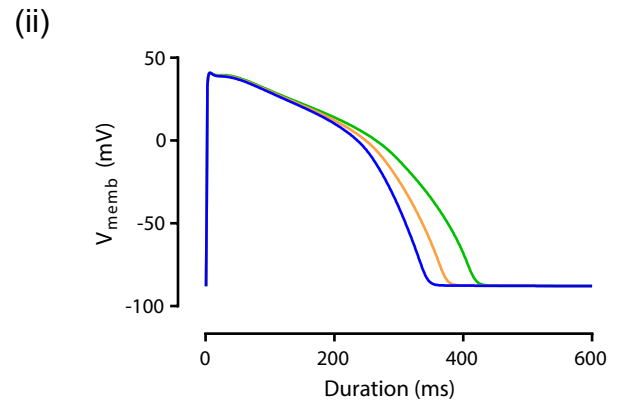
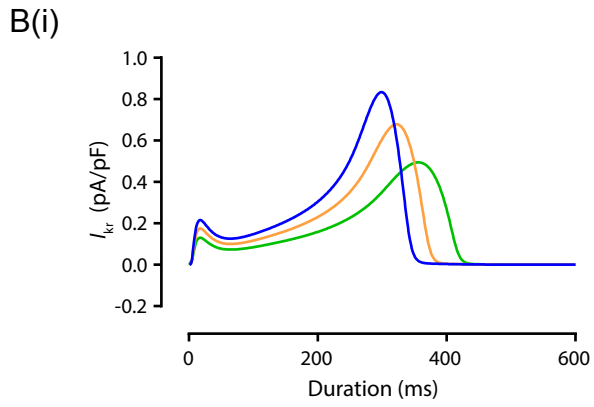
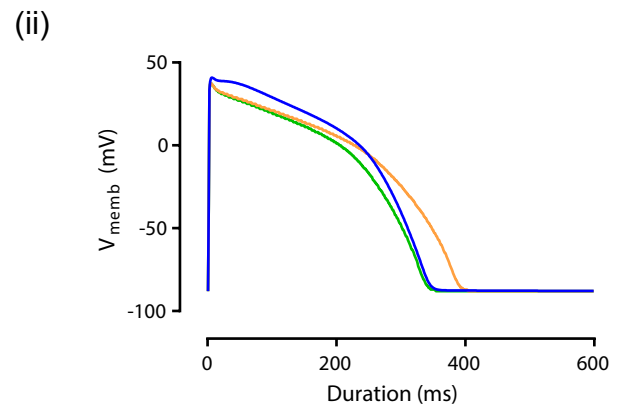
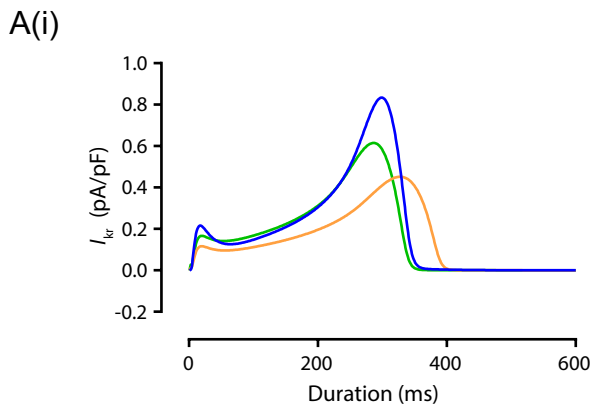
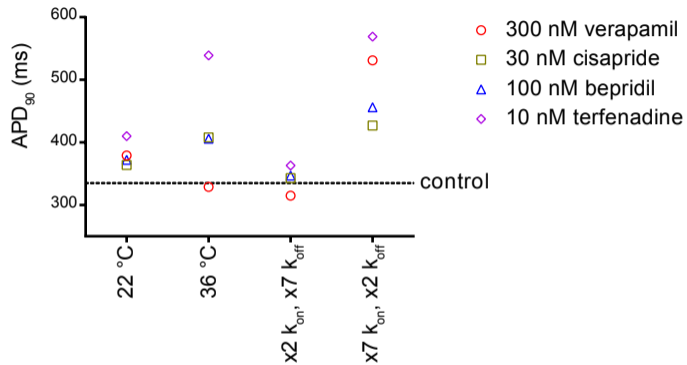


Figure 4

A



B

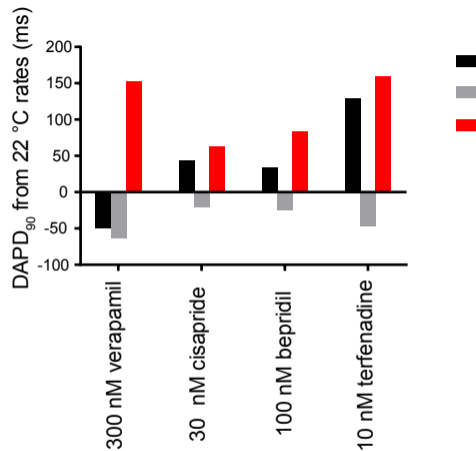


Figure 5